

# Low pressure chemical vapor deposition of massive $\text{Si}_{1-x}\text{Ge}_x$ gradient crystals and applications in short-wavelength diffraction

R. Madar and E. Mastromatteo

LMGP-ENSPG, BP 46, 38402 St Martin d'Hères (France)

A. Magerl and K.-D. Liss

ILL, 156X, 38042 Grenoble (France)

C. Bernard

LTPCM-ENSEEG, BP 75, 38402 St Martin d'Hères (France)

## Abstract

Bragg reflection from single crystals is commonly applied to define monochromatic beams in neutron and X-ray scattering. In general, mosaic crystals provide a significantly higher particle flux than perfect crystals, at the expense of a deterioration in the beam divergence. This disadvantage can be overcome by using gradient crystals, which are characterized by a continuous variation in the crystal lattice spacing. Diffraction from a gradient crystal can be described by simple mirror reflection for a desired wavelength band.

We synthesized various  $\text{Si}_{1-x}\text{Ge}_x$  single crystals with both fixed and continuously varying concentrations. They were grown on silicon substrates from a mixture of  $\text{SiH}_4$ ,  $\text{GeH}_4$ ,  $\text{H}_2$ ,  $\text{HCl}$  in a low pressure chemical vapor deposition reactor. The lattice spacing gradient was obtained by controlled variation of the gas flows. The various characterization techniques employed emphasize in particular the aspects of growth rate, crystallinity and mixing of the components. A test on a neutron diffractometer of a 0.85 mm thick crystal, grown for 24 h, showed the expected performance.

## 1. Introduction

Crystal monochromators are used to select or analyze energy in neutron and X-ray scattering [1]. Although one obtains the best resolution with perfect crystals, the reflected intensity is increased rapidly by using imperfect crystals. The imperfections lead to either a relaxation of the angular definition of crystal planes (mosaic crystals) or a relaxation of the lattice spacing definition (gradient crystals). The increased intensity is related to an effective increase in the reflecting crystal volume. Bragg's law defines the energy selection as

$$k_i = k_f + G$$

where  $k_i$ ,  $k_f$  are the incident and reflected wavevectors respectively, and  $G$  is the reciprocal lattice vector for the crystal volume concerned. A distribution of  $G$  causes the reflection of neighboring wavevectors for both mosaic and gradient crystals. Figure 1(a) shows the case for an ideal mosaic crystal: the  $G$ -vectors, all of the same length, are inclined to each other with an angular distribution  $\eta$  around the mean direction. An incident phase-space element with a divergence  $\alpha$  is reflected to a deformed energy-dispersed phase-space element with a divergence  $2\eta + \alpha$ . In the case of a gradient crystal as shown in Fig. 1(b), the  $G$ -vectors are parallel to each

other, but show different lengths. Thus, an incident phase-space element keeps its shape after reflection, *i.e.* the beam divergence remains  $\alpha$ , and there is no dispersion between energy and direction. In other words, the accepted phase-space element is reflected as from a mirror.

The distribution in length of the  $G$ -vectors is achieved by varying the size of the unit cell as a function of the spatial coordinates  $r$  of the gradient crystal. That means for the real space lattice vectors  $d_{hkl}$  with Miller indices  $hkl$  and of a constant gradient  $g_{hkl}$

$$d_{hkl}(r) = d_{hkl}(0) \left[ 1 + \frac{g_{hkl} r}{|d_{hkl}(0)|} \right]$$

$g_{hkl}$  is the gradient corresponding to  $d_{hkl}$  and for a cubic lattice transforms in the same way as  $d_{hkl}$

$$(h^2 + k^2 + l^2)^{1/2} |g_{hkl}| = (m^2 + n^2 + o^2)^{1/2} |g_{mno}|$$

Lattice spacing gradients can be obtained in various ways, for example by imposing a temperature profile on a thermally dilating material or, as in our case, by varying the composition of an alloy. Silicon-germanium compounds ( $\text{Si}_{1-x}\text{Ge}_x$ ) are interesting candidates. First, they can be mixed over the entire concentration range  $x$ . Second, the elements have the same lattice structure (diamond lattice). Starting from a pure silicon crystal,

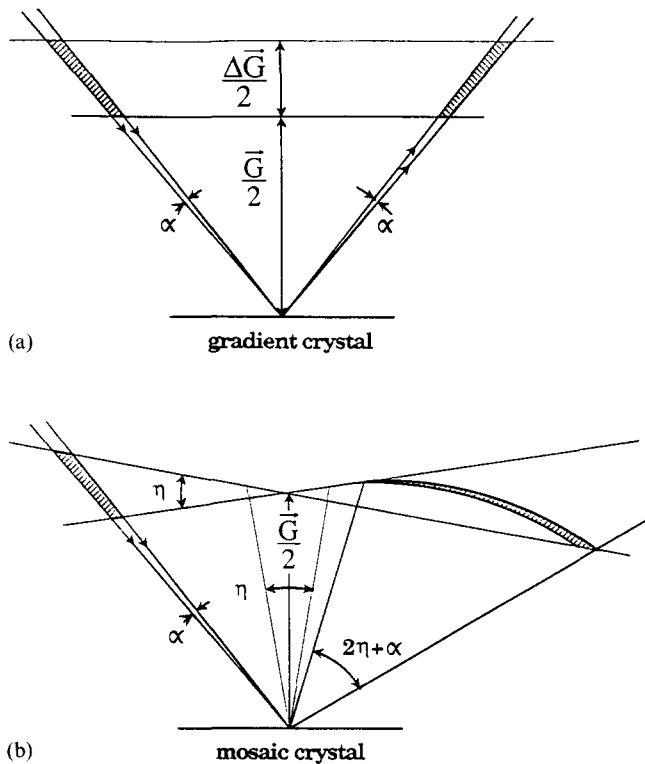


Fig. 1. Reflection diagrams for neutrons in reciprocal space for a mosaic crystal (a) and a gradient crystal (b).

silicon atoms are progressively replaced substitutionally by germanium atoms. The first point assures that the germanium sites are statistically distributed over the silicon lattice without formation of clusters. Third, the lattice constant of pure germanium ( $a_0(\text{Ge}) = 5.658 \text{ \AA}$ ) is 4.2% larger than that of pure silicon ( $a_0(\text{Si}) = 5.431 \text{ \AA}$ ). It has been shown that the average lattice spacing of an  $\text{Si}_{1-x}\text{Ge}_x$  alloy varies linearly with germanium concentration  $x$

$$a_0(\text{Si}_{1-x}\text{Ge}_x) = (1-x)a_0(\text{Si}) + xa_0(\text{Ge})$$

$a_0$  being the edge length of the unit cell.

## 2. Crystal growth

So far, attempts to grow single crystals of  $\text{Si}_{1-x}\text{Ge}_x$  directly from the melt have been without success. In fact, the first high-quality epitaxial layers of these alloys on silicon substrates were obtained by molecular beam epitaxy [2, 3] and very low pressure chemical vapor deposition (CVD) [4, 5] for use in integrated circuit technology. In an alternative approach, we synthesize them by low pressure chemical vapor deposition (LPCVD). A silane ( $\text{SiH}_4$ )-germane ( $\text{GeH}_4$ ) gas mixture streams over a heated silicon substrate. The  $\text{SiH}_4$  and  $\text{GeH}_4$  molecules which contact the hot surface (1320 K)

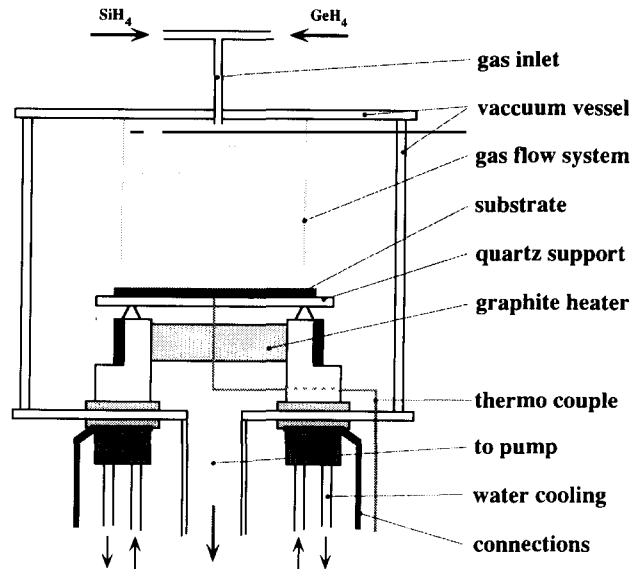


Fig. 2. Sketch of our LPCVD furnace.

crack, freeing silicon or germanium atoms for epitaxial deposition onto the substrate.

The germanium concentration of the crystal depends on the  $\text{GeH}_4$  concentration in the gas mixture, which is easily controlled. Figure 2 shows a sketch of the LPCVD furnace. A quartz stand ( $\varnothing = 150 \text{ mm}$ ) to hold the silicon wafer ( $\varnothing = 100 \text{ mm}$ ) is located inside a water-cooled vessel of stainless steel ( $\varnothing \approx 30 \text{ cm}$ ,  $h \approx 30 \text{ cm}$ ). The substrate is heated from below by a graphite resistor. A thermocouple near the wafer monitors the process temperature.

There are four process gas lines: 1%  $\text{SiH}_4$  in argon, 1%  $\text{GeH}_4$  in argon,  $\text{H}_2$  and  $\text{H}_2\text{-HCl}$  respectively. Each line is equipped with an electronically controlled mass flowmeter. The gases are brought to a mixing chamber and guided to the top of the LPCVD vessel. Inside the reaction chamber, the gas jet is dispersed homogeneously over the substrate surface. The pressure inside the vessel is regulated via pumps and control valves on the exhaust line. Before growth, the wafers are subjected to a high temperature  $\text{H}_2$  bake at 1450 K for 5 min followed by an  $\text{H}_2\text{-HCl}$  etch at the same temperature for 2 min to remove the native oxide. The growth starts with epitaxial deposition of pure silicon. Progressive introduction of  $\text{GeH}_4$  in the gas stream leads to the formation of graded layers with increasing germanium concentration. Typical process parameters are 1320 K for the deposition temperature and a pressure of about  $p = 150 \text{ Pa}$ . Growth rates of  $0.7 \mu\text{m min}^{-1}$  have been achieved under these conditions.

## 3. Experimental crystal growth

The first results were obtained on small-sized samples ( $2 \text{ cm} \times 2 \text{ cm}$  Si[100] wafers), used to optimize process

parameters as well as surface preparation of the substrates. Crystals with both stepped (step crystal) and continuous variation in germanium concentrations (gradient crystals) were made.

The results of a microprobe analysis are shown in Figs. 3(a) and 3(b) for a step crystal and a gradient crystal respectively. These curves were obtained by scanning with a fine electron beam over the polished edge of a broken wafer.

The concentration  $x$  of the  $\text{Si}_{1-x}\text{Ge}_x$  crystal as a function of the concentration  $c(\text{GeH}_4)$  in the gas phase is shown in Fig. 4 for the step crystal. The germanium concentration  $x$  in the bulk is less than the corresponding concentration  $c(\text{GeH}_4)$  in the gas mixture with

$$x_{\text{step}} = 0.79c(\text{GeH}_4)$$

Evaluating the gradient crystal data, a slightly different relation is obtained:

$$x_{\text{gradient}} = 0.67c(\text{GeH}_4)$$

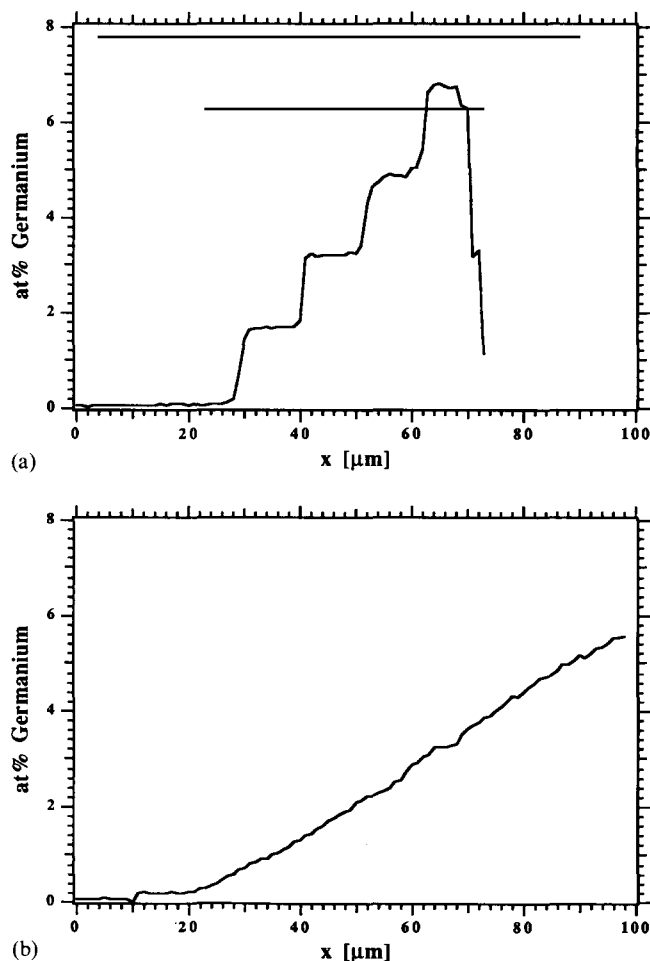


Fig. 3. Microprobe analysis of a step crystal (a) and a gradient crystal (b). The growth time was 20 min for each step, total 100 min in case (a) and 180 min in case (b).

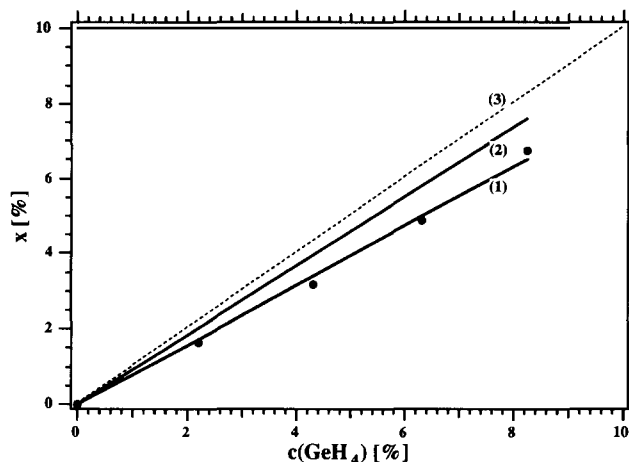


Fig. 4. Germanium concentration  $x$  of an  $\text{Si}_{1-x}\text{Ge}_x$  step crystal as a function of the germane concentration in the gas phase: curve 1, experimental; curve 2, results of the thermodynamic calculations; curve 3, ideal curve corresponding to total decomposition of the reactive gases.

This difference in slope can be explained by the time constant for changing the gas composition in the reactor chamber.

This systematic deviation of the layer composition relative to the  $\text{GeH}_4:\text{SiH}_4$  ratio in the gas phase has already been found and discussed in other reports on CVD of these materials. Thermodynamic equilibrium calculations [6, 7] show indeed that the introduction of chlorine atoms in the system (from intentionally introduced HCl or resulting from the decomposition of  $\text{SiH}_2\text{Cl}_2$  [8]) leads to a decrease in the germanium content of the deposited layer compared with the ideal value (Fig. 4). However, the experimental value is far below the calculated value, which means that any modeling of this process must include the fluid mechanics of the gas phase in the description of experimental conditions and some hypothesis of the deposition kinetics. This work is in progress.

Figures 5(a) and 5(b) show optical micrographs of the surfaces of a [100]-oriented and a [111]-oriented crystal respectively. As expected from the symmetry of the crystals, squares are observed for [100] and triangles for [111] wafers. These well defined structures indicate epitaxial crystalline growth.

For neutron and X-ray scattering, gradient crystals with a thickness in the centimeter range are necessary. An estimation for this is given later. To obtain such thick crystals, the growth rate is a very important aspect and should be of the order of  $0.7 \mu\text{m min}^{-1}$  ( $117 \text{ \AA s}^{-1}$ ). The growth rate can be readily determined by weighing the wafer before and after crystal growth. Alternatively, microprobe measurements on step crystals as shown in Fig. 3(a) can be used. Figure 6 shows the experimental growth rate as a function of the process temperature

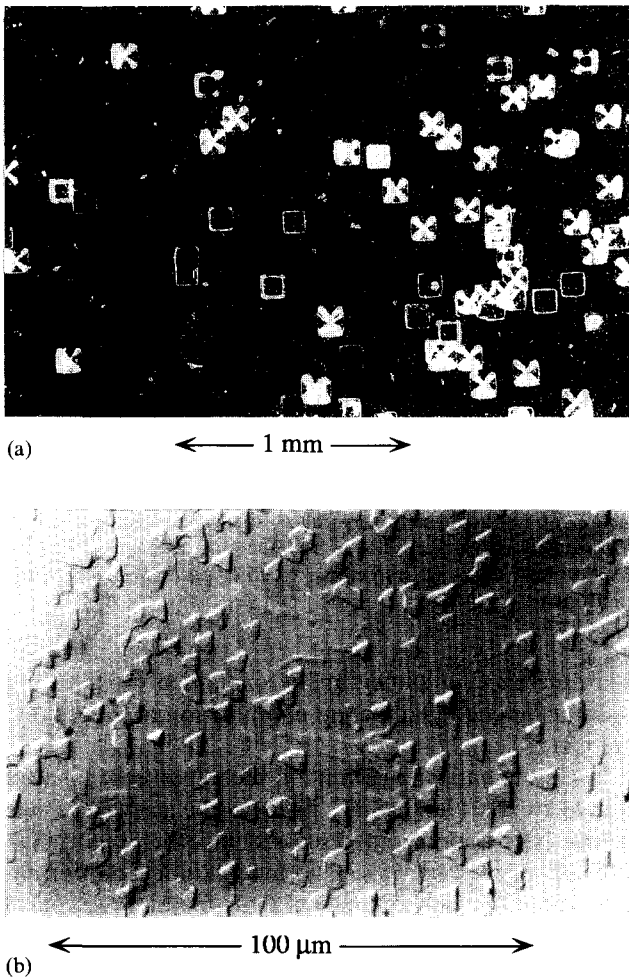


Fig. 5. Pictures of a [100] surface (a) and a [111] surface (b) of crystals grown by our LPCVD technique. They show structures corresponding to the crystal symmetry.

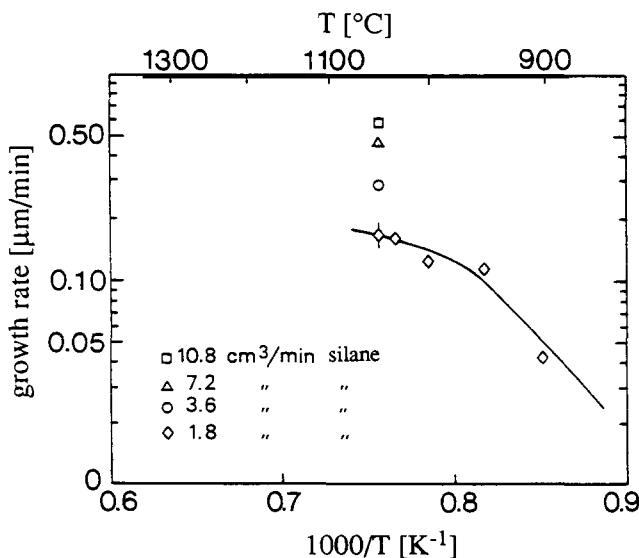


Fig. 6. Crystal growth rate as a function of temperature and silane flux.

and  $\text{SiH}_4$  flux. In general, a higher temperature as well as higher flux increases the growth rate. The aim of  $0.7 \mu\text{m min}^{-1}$  has been reached under favorable conditions (gas flux, temperature, pressure). During 24 h, two gradient crystals with thicknesses of about 0.85 mm were grown.

#### 4. Neutron diffraction

The gradient of the crystals must be optimized with respect to a particular crystal reflection and neutron wavelength. The reflection curve of a perfect crystal in the Bragg geometry is known as a Darwin curve. Usually, it is plotted as a function of a dimensionless parameter  $y$ , which may be simply explained as the half-width of the Darwin plateau.  $y$  is directly proportional to the lattice parameter variation, which is

$$\delta d/d = 9.15 \times 10^{-6} y$$

for neutrons and Si[111].

A characteristic crystal thickness  $\Delta_0$  is necessary to approach the ideal shape of this curve. The basis of an optimal gradient crystal assumes a change in lattice parameter  $d$  by  $\Delta d/d = \Delta\lambda/\lambda$  within a thickness  $\Delta_0$ , where  $\Delta\lambda/\lambda$  denotes the natural width of the Darwin curve. In other words, the position of Darwin curves for neighboring crystal volumes which have a thickness  $\Delta_0$  are shifted by the gradient corresponding to their own widths  $\Delta\lambda/\lambda$ .

Thus, the reflectivity of these optimized gradient crystals rises to a saturation value of 100% inside a range  $\delta\lambda/\lambda = gD/d$ ,  $D$  being the thickness of the gradient crystal. If the gradient  $g$  is too large, the lattice spacing varies too rapidly and too few lattice planes interfere for a given wavelength. Consequently the intensity decreases. However, if  $g$  is too small, primary extinction occurs preventing a portion of the crystal volume from contributing to the reflectivity. Valuable crystal volume is wasted even in the case of absorption-free crystals. For the Si[111] reflection,  $\Delta_0 = 34 \mu\text{m}$ . Thus crystals with a thickness of several millimeters are necessary for the reflectivity to increase several hundred times.

Figures 7(a) and 7(b) show experimental results from a gradient crystal and a perfect silicon crystal respectively. These data were measured on a neutron back-scattering spectrometer. The scan was performed parallel to the reflecting Si[111] reciprocal lattice vector. The figures show the transmitted intensity as a function of  $y$ .

#### 5. Results for neutron diffraction

The measured line width of the gradient crystal is  $y_B = 150$ , ( $\delta d/d = 1.4 \times 10^{-3}$ ), i.e. 75 times larger than a

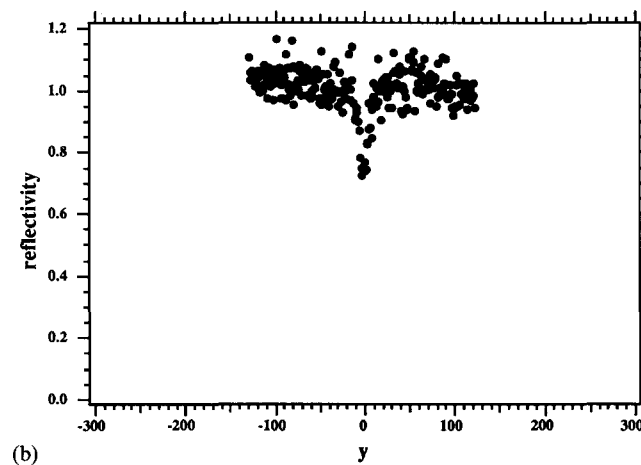
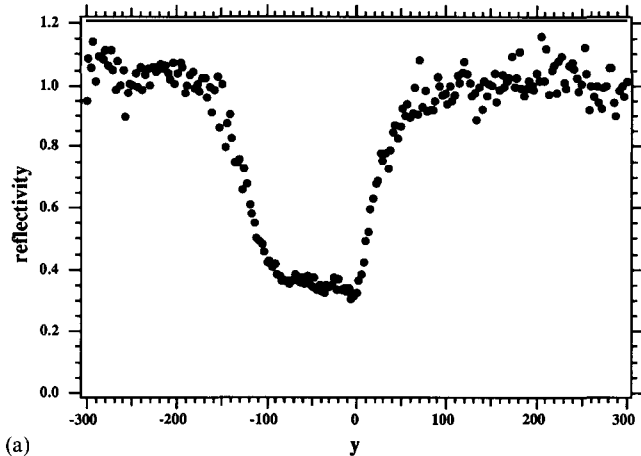


Fig. 7. Neutron backscattering spectra in transmission of a gradient crystal (a) compared with a perfect crystal (b). Note the box-like shape of (a) which differs strongly from a gaussian line.

perfect Si[111] reflection. The value for the integrated reflectivity of 98 on the  $y$  scale is 31 times higher than the corresponding value for an ideal crystal. The peak reflectivity is about 65%.

The perfect silicon reference peak shows a small dip. Its width is large compared with the calculated value. This is due to the finite resolution of the spectrometer.

Its integrated reflectivity, however, is 3.18, which is very close to the theoretical value of  $\pi$ .

## 6. Discussion

The neutron backscattering data reflect the gradient in the lattice parameter spacing well. The intended gradient is about three times steeper than for the ideal case. In fact, the measured  $\delta d/d$  and the total crystal thickness of  $D=0.85$  mm lead to an effective crystal volume of approximately  $\Delta_0/3$ . Thus the expected peak reflectivity is approximately 75%, which is in fair agreement with the measured value of 65%.

## 7. Conclusion

We have demonstrated the feasibility of growing thick  $\text{Si}_{1-x}\text{Ge}_x$  gradient crystals by LPCVD with very high growth rates of up to  $0.7 \mu\text{m min}^{-1}$ . The composition and the quality of the single crystals have been carefully analyzed. Their diffraction properties are well understood and they offer novel applications in both neutron and short-wavelength X-ray optics.

## References

- 1 A. Boeuf, P. Detourbet, A. Escoffier, R. Hustache, S. Lagomarsino, A. Reunert and F. Rustichelli, *Nucl. Instrum. Methods*, 152 (1978) 415.
- 2 J. C. Bean, T. T. Sheng, L. C. Feldman, A. T. Fioty and R. T. Lynch, *Appl. Phys. Lett.*, 44 (1984) 102.
- 3 E. Kasper and H. J. Herzog, *Thin Solid Films*, 44 (1977) 357.
- 4 B. S. Meyerson, K. J. Uram and F. K. Legoues, *Appl. Phys. Lett.*, 53 (1988) 2555.
- 5 G. L. Patton, J. H. Comfort, B. S. Meyerson, E. F. Crabbee, G. J. Scilla, E. de Fressard, J. M. C. Stork, J. Y. C. Sun, D. L. Haramé and J. N. Burghartz, *IEEE Electron Devices Lett.*, 11 (1990) 171.
- 6 H. P. Tang, L. Vescan and H. Lüth, *J. Cryst. Growth*, 116 (1992) 1.
- 7 H. Rouch, R. Madar and C. Bernard, to be published.
- 8 T. I. Kamins and D. J. Meyer, *Appl. Phys. Lett.*, 59 (2) (1991) 178.